Accepted Manuscript

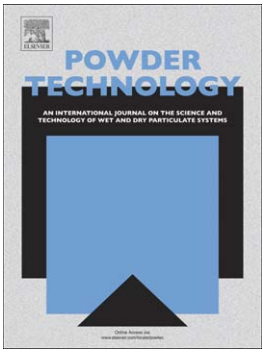

Synthesis of natural porous minerals supported TiO_2 nanoparticles and their photocatalytic performance towards Rhodamine B degradation

Bin Wang, Guangxin Zhang, Zhiming Sun, Shuilin Zheng

PII: S0032-5910(14)00358-1
DOI: doi: 10.1016/j.powtec.2014.04.050
Reference: PTEC 10211

To appear in: *Powder Technology*

Received date: 19 February 2014
Revised date: 9 April 2014
Accepted date: 11 April 2014

Please cite this article as: Bin Wang, Guangxin Zhang, Zhiming Sun, Shuilin Zheng, Synthesis of natural porous minerals supported TiO_2 nanoparticles and their photocatalytic performance towards Rhodamine B degradation, *Powder Technology* (2014), doi: 10.1016/j.powtec.2014.04.050

Synthesis of natural porous minerals supported TiO_2 nanoparticles and their photocatalytic performance towards Rhodamine B degradation

Bin Wang [a, b], Guangxin Zhang [a], Zhiming Sun [a], Shuilin Zheng [a, *],

[a] *School of Chemical and Environmental Engineering, China University of Mining & Technology, Beijing 100083, PR China,*

[b] *School of Chemistry and Molecular Biosciences, The University of Queensland, Brisbane Qld 4072, Australia*

Email: shuilinzheng8@gmail.com, wangbin0710@hotmai.com,

Tel: +86 10 62390972

Abstract Natural porous minerals supported (TiO_2/diatomite) photocatalyst was prepared via a modified sol-gel method using titanium (IV) butoxide (TBOT) and diatomite. The effect of TBOT dosage on adsorption capacity and photocatalytic activity for Rhodamine B (RhB) solution was investigated. The morphology and elemental distribution were determined by scanning electron microscopy with attached energy-dispersive X-ray detector. The porous and crystalline structures were characterized using nitrogen adsorption-desorption and X-ray diffraction techniques, respectively. The prepared TiO_2/diatomite hybrid catalyst has shown relatively even porous structure and dispersion of TiO_2 over the surface. This suggests that the diatomite matrix prevented the agglomeration of TiO_2 particles. Initially, the surface area and pore volume of the hybrid catalyst were increased by adding TBOT then decreased for dosages higher than 1.0 ml. The crystalline size of TiO_2 immobilized on diatomite matrix by sol-gel method was around 20 nm. When the experiments were carried out in absence of diatomite this value was increased to 33.73 nm. The use of diatomite also promoted an increase of the transformation temperature of the crystalline phase anatase to rutile for the TiO_2. The as-prepared TiO_2/diatomite composite exhibited high photocatalytic activity (96.0% for 0.5 h UV-light irradiation) for the degradation of RhB from wastewater as a result of its unique porous structure and optimum TiO_2 loading. In addition, it can be easily separated from suspension and possess a good durability. This hybrid material holds great promise in the engineering field for the environmental remediation.

Key words: Titanium dioxide; Diatomite; Sol-gel; Durability

1. Introduction

Along with the enhancement of environmental protection consciousness and the improvement of global environmental standards, environmental pollution control has received enormous attention. In recent decades, researchers have focused on finding an environmentally friendly and economical method that can degrade organic components from industrial and municipal effluent. Various catalytic techniques have been applied in the field of environmental protection. Among these, TiO_2 heterogeneous photocatalysis as a promising technology that stands out and has been effectively exploited for the complete mineralization of dyes, insecticides and indoor volatile organic compounds (VOCs) [1-3], owing to its high photocatalytic activity, biological and chemical inertness and non-toxic nature [4]. However, the practical application of nanosized TiO_2 materials in the pollutants elimination suffers from several difficulties, such as agglomeration, separation and recovery of fine catalyst particles [5]. And also, poor adsorption property leads to great limitation in exploiting its best

photo-efficiency. In order to figure out these problems, there have been many reports of improving the photo-efficiency of TiO_2 by immobilizing it on adsorbents like silica [6, 7], active carbon [8], zeolite [9] and clays [10-12], which have a large surface area and/or porous microstructure. These results show that the introduction of adsorbent support not only immobilize and disperse TiO_2 particles on adsorbents but also induce a synergistic effect because of the adsorption with respect to organic molecules.

Nano-TiO_2/Clay composites have been postulated as suitable alternative photocatalyst in environmental remediation. In particular, for low concentration condition, these materials offer a large porous structure to adsorb pollutants molecule due to a high adsorption capacity [13]. Porous non-metal mineral is an important series of clay materials, which is widely used as support since its large specific surface area, high porosity and abundant reserves, such as hectorite [10-12], diatomite [14-16], palygorskite [17, 18], etc. Among these, diatomite has been used extensively as filtration media, adsorbents, and conventional catalyst supports [19]. As there are a lot of silicon hydroxyls and hydrogen bonds on the surface of diatomite, it can form strong force with nano-TiO_2, inhibiting TiO_2 to be washed away in flow system and subsequently improving system photo-efficiency. Additionally, nano-TiO_2 immobilized on diatomite combines large specific surface area of diatomite with excellent photoactivity of TiO_2. Therefore this hybrid catalyst not only solves the issues of aggregation and recovery of nano-TiO_2 in suspension system but also enlarges the irradiation surface of TiO_2 and increases light utilization rate. Simultaneously, photocatalysis is a surface process; therefore, the structural properties and the surface coverage of active sites are crucial for photocatalytic efficiency. In order to give full play to the adsorption property of diatomite and photocatalytic activity of nano-TiO_2, we should strictly control the distribution of TiO_2 on the surface and protect porous structure from blocking by TiO_2 aggregated bulk.

In this work, our interests focus on adsorption and photocatalytic abilities for organic dye over TiO_2/diatomite hybrid catalyst in aqueous solution. We aim to synthesize a promising titania nanostructure that behaves both as high porosity as natural diatomite and as efficient photocatalysis as TiO_2 by using a modified sol-gel method. Furthermore, aiming to avoid an ineffective excess of catalyst and to ensure a total adsorption of efficient photons, the optimum loading of TiO_2 needs to be found. To examine the adsorption/photocatalysis capability of the hybrid TiO_2/diatomite samples, a well-known dye, Rhodamine B (RhB), was employed here. We discovered two pathways for removal of dye on porous TiO_2/diatomite: adsorption and UV-light derived photocatalysis, which indicated broad prospect in effluent treatment and greening indoor adornments. In contrast to conventional TiO_2 photocatalyst (Degussa P25), the nano-TiO_2/diatomite particles we obtained can be easily separated and display good durability after five reaction cycles.

2. Experimental

2.1 Preparation of TiO_2/diatomite hybrid catalysts

The raw diatomite (Jilin province, China) was used as catalyst carrier after purified. The purified process has been described in detail elsewhere [20]. The chemical compositions of the purified diatomite (DE) are listed in **Table 1**. As summarized in **Table 1**, it is clear that the main chemical composition of porous diatomite mineral is amorphous SiO_2. Titanium (IV) butoxide (TBOT, ≥97%, Aldrich), glacial acetic acid (CH_3COOH, Ajax Finechem Pty Ltd), ethanol (C_2H_5OH, Merck Germany) and hydrochloric acid (HCl, 36%, Ajax Finechem Pty Ltd) were used as received without any further

purification process. Degussa P25 (Dusseldorf, Germany) consists of 75% anatase and 25% rutile with a specific BET-surface area of *ca*. 50 m^2/g and primary particle size of 20 nm was used as a reference. Rhodamine B (RhB) dye was used as a model contaminant in the photocatalytic activity measurements. Deionized water was used throughout all experimental procedures.

The preparation of TiO_2/diatomite hybrid composites was undertaken by a modified sol-gel method as shown in **Fig.1**. Firstly, 1 g DE dispersed in 14 ml of ethanol and 1 ml of acetic acid under stirring for 30 min to form diatomite suspension. Secondly, different dosages of TBOT were added dropwise in diatomite suspension under continuous stirring. Then, a solution was carried out by mixing ethanol and water with the pH value of *ca*. 2 through adding HCl. After that, this solution was added dropwise into suspension to arouse hydrolysis of TBOT at a moderate rate then forming the sol. The resulting mixture was stirred for 12 h to age and immobilize as-generated TiO_2 colloids on the surface of DE. Finally, the product was dried in oven at 105℃ for 4 h with subsequent calcination at 750℃ for 2 h in air at a heating rate of 2.5°/min. For comparison, different TiO_2 samples without diatomite were also prepared in same method and condition. In this study, the TiO_2/diatomite composites were denoted as TD-X listed in Table 2, respectively. In other words, X means the volume of TBOT as 0.5, 0.75, 1.0, 1.5, 2.0, 3.0 and 4.0 ml.

2.2 Characterization of TiO_2/diatomite hybrid catalysts

X-ray powder diffraction (XRD) patterns were taken on Bruker D8 advance diffractometer at 40 kV and 20 mA, using Cu Kα radiation at a scan rate of 4°/min. The average crystal sizes of the catalysts were determined according to the Debye-Scherrer equation using FWHM data after correcting for the instrumental broadening. The surface morphology was observed with scanning electron microscopy (SEM, EVO 18 Carl Zeiss) performed at 10.0 kV with attached energy-dispersive X-ray (EDX) detector to perform the elemental analysis. The Brunauer-Emmett-Teller (BET) surface area (S_{BET}) was determined by nitrogen adsorption-desorption isotherm measured at -196 ℃ (ASAP 2020) and Barret-Joyner-Halender (BJH) method was applied to obtain pore size distribution, respectively.

2.3 Adsorption/photocatalysis of TiO_2/diatomite hybrid catalysts

The photocatalytic activity of as-prepared composites were assessed in terms of the degradation of RhB in aqueous solutions using a 250 W high-pressure mercury lamp (λ=365 nm) as UV-light source. For the degradation of RhB, 0.05 g of Degussa P25 or as-prepared composites was dispersed in 100 ml of standard RhB aqueous solution (10 mg/l) and underwent ultrasonic treatment for 10 min to form stabilized suspension. The suspension consisting of photocatalyst with different TBOT dosage and RhB were added into a cylindrical reactor under constant magnetic stirring. Prior to UV illumination, the suspension was stirred for 1 h in dark, in order to establish the adsorption-desorption equilibrium between RhB and the catalyst, followed by irradiation for 1 h with UV-light. In the definite intervals, the sample of suspension (*ca*. 4 ml) was withdrawn from the reactor and centrifuged to remove the photocatalyst particles. Then the photocatalytic discoloration of RhB was analyzed by UV-vis spectrophotometer (UV-9000S, Shanghai Yuanxi) through measuring the adsorption spectra change at 562 nm. The fractional degradation efficiency (D_R) of RhB was calculated by the following equation:

$$D_R(\%) = \frac{(C_0 - C_t)}{C_0} * 100 \qquad \text{Eq. (1)}$$

where C_0 is the initial concentration of RhB and C_t is the concentration at definite interval of time, respectively. The durability of as-prepared catalyst for the degradation of RhB solution was tested under the same condition by running the reaction for five cycles. The initial concentration of RhB in

suspension was kept at 10 mg/l. At the end of every cycle, the re-collected particles were washed several times using ethanol and deionized water till the residue solution was clear, and then dried in an oven for 4 h at 105℃.

3. Results and discussion

3.1. SEM/EDX analysis

The SEM morphologies of raw diatomite and purified diatomite are shown in **Fig. 2a** and **b**. The SEM image of raw diatomite shows a disc-like shape with diameter of *ca*. 20-30 μm. But there are some impurities on the surface of diatom, which block partial pores. **Fig. 2b** shows the characteristic disc-like shape of diatom after purification is still kept integrality with nearly regular array of submicron pores in diameter of *ca*. 500 nm. The pores on the surface of diatom could be seen more clearly after purification, which might be due to the fact that the impurities were removed from the clogged pores. The morphology changes during deposition are also clearly revealed by SEM as shown in **Fig. 2c-f**. After the deposition and relatively high temperature calcination (750℃) the disc-like shape and porous structure of the diatomite are both well preserved. Moreover, compared to the clean surface of purified diatomite (**Fig. 2b**), the TD-X (X=0.5, 1.5, 2.0 and 3.0) samples (**Fig. 2c-f**) were apparently rougher. After adding 0.5 ml TBOT, small TiO_2 nanoparticles can be observed on the surface. Furthermore, with increasing volumes of TBOT up to 3.0 ml, the larger nanoparticles were obtained and a part of them blocked the pores, which will lead to a shielding effect on the light transmittance and pollutants adsorption. Then, the number of charge carrier generated on the irradiated TiO_2 probably reduced, consequently the amount of the interfacial charge transfer to adsorbed substrates would also decrease. At the same time, the surface of TD-3.0 became much rougher than that of TD-0.5. The inset of **Fig. 2d** represents the distribution of titanium measuring by EDX under surface-distribution scanning. It clearly indicates the homogeneous distribution of TiO_2 nanoparticles on diatomite surface, although several of them tend to agglomerate and block the pores. This result suggests that the current immobilized catalyst preparation method allows homogenous and intimate loading of TiO_2 nanoparticles onto diatomite to form a stable hybrid photocatalyst. We also used quantitative district analysis to illustrate the composition both in weight and atomic percentage of the silicon, titanium and oxygen, as summarized in **Table 2**. The rest of the components, such as carbon, palladium and gold involved by sample preparation, were normalized. With the increasing TBOT dosage, the weight and atomic percentage of titanium increased. However, the increment of these two percentages was not proportional to TBOT dosage. This is maybe attributed to that a little part of titanium didn't load onto diatomite.

3.2 N_2 adsorption

The effect of TBOT dosage on the surface area and pore structure parameters were studied by measuring various TiO_2/diatomite samples using nitrogen adsorption-desorption isotherm and BJH pore size distribution. **Fig. 3a** and **b** show the N_2 adsorption-desorption isotherms and the corresponding pore size distribution curves of DE and TD-X (X=0.5, 1.0, 1.5, 2.0 and 3.0) samples. The results of BET surface area (S_{BET}), pore volume and average pore diameter were summarized in **Table 3**. **Fig. 3a** exhibits these isotherms of TD-X have a hysteresis behavior within high relative pressure of 0.65~0.99, being representative of mesoporosity in the all samples [21, 22]. The adsorption capacity first increases and then decreases with the increase in TBOT dosage, and TD-0.5 has the

largest S_{BET} (18.84 m^2/g). Whilst all coated samples have a larger S_{BET} than that of DE (5.57 m^2/g), indicating marked agglomeration does not occur that destroy the porous structure of TiO_2/diatomite prepared by this method. Large surface area with mesoporous structure can promote adsorption, desorption and diffusion of reactants and products, which is favorable to obtain a high photocatalytic activity [22-26]. The pore size distributions in **Fig. 3b** show that TD-1.0 and TD-1.5 samples had narrow pore size distributions with the average pore diameter at *ca*. 11.32 and 11.83 nm respectively. However, DE had wide pore size distribution and big pores with an average diameter of 17.77 nm, because the pore size in diatomite decreased from boundary to center. With increasing TBOT dosage up to 3.0 ml, the accumulation of TiO_2 crystal on the surface resulted in the decrease of BJH desorption cumulative volume of pores and average pore diameter. Both the variation of these two pore structure parameters are correlated to the crystallite growth and partial agglomeration that damage porous structure of diatomite. In a word, the variation of surface area and pore structure parameters for hybrid TiO_2/diatomite catalysts as measured by N_2-sorption was ascribed to the variation of TBOT dosage in preparing process.

3.3 X-ray diffraction

The structural patterns of DE and TiO_2 coated diatomite samples were studied using X-ray diffraction. The crystalline phases and crystalline sizes for TiO_2 coated diatomite samples with different TBOT dosages are given in **Fig.4** and **Table 3**. The XRD pattern of DE is in good agreement with that of the referenced amorphous opal-A, which is characteristic of a broad diffraction peak centered at around 2 θ =21.8˚ [27]. And there are two characteristic diffraction peaks at 2 θ =21.4˚ and 27.2 ˚ corresponding to Quartz. All the XRD patterns of diatomite-supported TiO_2 particles show the obvious peaks relating to anatase phase (JCPDS 21-1272) at 2 θ =25.8 ˚ (101), 38.4 ˚ (004) and 48.8 ˚ (200), and the peaks become sharpen and strengthen with increasing dosage. Compared to pure TiO_2 prepared by sol-gel method [28-30], there is no existence of diffraction peak for rutile phase in hybrid samples even when the calcination temperature reached 750℃. We can infer that the involvement of diatomite into hybrid photocatalyst can effectively postpone the crystalline phase transformation from anatase phase to rutile phase in TiO_2, which is endorsed by thermal stability and increases photocatalytic activities [31]. Based on the full width half maximum (FWHM) of pattern peaks and Debye-Scherrer equation, the average crystalline sizes of anatase and rutile were calculated and listed in **Table 3**. With the increase in TBOT dosage, crystalline size of anatase increases from 14.65 nm of TD-0.5 to 23.73 nm of TD-3.0, which also results in a slight broadening in XRD peaks. Moreover, comparing with TD-3.0, T-3.0 (pure TiO_2 sample without support prepared under the same condition in this work) shows a different crystalline structure with larger anatase size (33.73 nm) and presence of rutile phase when calcination at 750℃ (plot "T-3.0" in **Fig.4**). This is because TiO_2 crystallites tend to agglomerate originating bigger crystal particles with subsequent transformation from anatase phase to rutile phase [32]. And then it is suggested that the support improves the distribution of TiO_2 particles and impedes the formation of aggregation.

3.4 Adsorption and Photocatalytic performance of TiO_2/diatomite catalyst

The loading amount of TiO_2 onto diatomite not only has a significant influence on surface morphology, crystalline structure and porous structure of hybrid catalyst but also on adsorption and photocatalytic activity in terms of the degradation of dye RhB, as shown in **Fig.5**. **Fig. 5a** shows the

variation plots of RhB concentration in the absence and presence of TiO_2/diatomite as well as Degussa P25. Before turning on the lamp, a dark adsorption step has been launched for 1 h to make sure RhB molecules reaching adsorption-desorption equilibrium between TiO_2/diatomite composites. After turning on the lamp, curve "Blank" in **Fig. 5a** suggests that degradation of RhB was very slow without catalyst (only *ca*. 5% decomposition after 1 h irradiation). The sample DE displayed a removal ratio of RhB with *ca*. 8% in 0.5 h irradiation, whereas within the same time interval, samples TD-X (X=0.5, 1.0, 1.5 and 3.0 ml) showed 91.4%, 95.6%, 96.0% and 84.0% degradation efficiency respectively. And all the composite samples showed more than 75.5% degradation efficiency as high as Degussa P25. On the other hand, as shown in **Fig. 5b,** all the photocatalytic degradation profiles (after turning on the lamp) could be correlated with the following pseudo-first order kinetic model with good agreement, which could be well explained in terms of the Langmuir-Hinshelwood mechanism [32-34].

$$ln\left({C}/{C_0}\right) = -kKt = -k_{app}t \qquad \text{Eq. (2)}$$

where C is the concentration of the RhB (mg/l), C_0 is the initial concentration of the RhB (mg/l), t is the illumination time (min), k is the reaction rate constant (mg/l min), K is the adsorption coefficient of the reactant (l/mg) and k_{app} is the apparent rate constant (min^{-1}). The plots of $-\ln(C/C_0)$ versus irradiation time (t) for different samples are shown in **Fig. 5c** (in consideration of conciseness, we only provided four plots). All kinetic plots are linear, which confirms that the photodegradation reaction of RhB on TiO_2/diatomite is well fitted to the pseudo-first order reaction kinetics. The k_{app} values for hybrid catalysts were estimated from the slop of these linear plots and summarized in **Table 4**. It was found that, as the TBOT dosage increased from 0.5 to 3.0 ml, the degradation efficiency of RhB and k_{app} first increased and then decreased notably. The reaction rate increased from 6.34×10^{-2}/min in the presence of TD-0.5 to 9.38×10^{-2}/min for TD-1.5 and then decreased to 5.05×10^{-2}/min for TD-3.0. Thus the optimum loading dosage of TBOT is *ca*. 1.5 ml in this work. The kinetic model shows that the sample with optimum TBOT dosage has twice higher photocatalytic activity than that of the sample with excessive loading. It is possible that the initial increase could be associated to an increment of photoactive components which can be stimulated under UV irradiation and generated radicals to react with RhB molecules [24]. However, continual increase in the catalyst loading to 3.0 ml resulted in reduction both in the degradation efficiency and in the apparent rate constant. This can be assigned to the aggregation of overmuch TiO_2 nanoparticles that possibly block the pores of diatomite (**Fig. 2f**) and accelerate the recombination of photo-generated holes and electrons between grains. This result is consistent with Hao et al.'s report [35] and their results indicated that the small particle size made the diffusion of photo-generated electron-hole pairs faster to the surface than in the large particle and resulted in falling recombination probability. Another reason may be due to this agglomeration makes a significant fraction of the active component are inaccessible to absorb neither the molecules nor the irradiation [26].

To investigate the relationship between dark adsorption and UV-light derived photocatalysis for RhB over TiO_2/diatomite catalyst, the equilibrium adsorption amounts (Q_e) of samples with different TBOT dosage were calculated by the following equation:

$$Q_e = \frac{V(C_0 - C_e)}{M\times1000} \qquad \text{Eq. (3)}$$

where C_0 and C_e are the initial and equilibrium concentrations of the RhB solution (mg/l), respectively, V is the volume of the RhB solution (ml), and M is the mass of sorbent (g). And the variation tendency

of equilibrium adsorption amount and apparent rate constant versus TBOT dosage is illustrated in **Fig. 5d** respectively. Since there was a decrease in S_{BET} with the increasing TBOT dosage, this could explain that the reduction of equilibrium adsorption amount of RhB on TiO_2/diatomite surface was derived from change of surface areas by TiO_2 coating. While when the dosage kept increased, the Q_e of RhB exhibited a little enhancement. This change of Q_e may be supported by the fact that the TiO_2 on hybrid catalyst exhibited slight adsorption abilities for RhB dye with the Cl^-, counter ion, by electrostatic attraction [24, 26] due to the reaction solution possesses weak acidity, which can compensate the disadvantage in surface area. In addition, it is found that the apparent rate constant didn't increase as the increasing adsorption amount, whereas it was decreasing in this case. This result is different from previous literatures [21, 22], Hsieh et al. synthesized Co-doped titania nanotubes and found that the adsorption and visible-light photocatalysis of BV10 were conformed to pseudo-second order kinetics and the photocatalysis became the rate-determining step during the adsorption/photocatalysis hybrid process. And the apparent rate constant for visible-light photocatalysis increased with the increasing dark adsorption capacity. But in our work under the UV-light irradiation, the photocatalytic degradation dominates the adsorption/photocatalysis process, which is similar with Hwang et al.'s and Liang et al.'s results [32, 36]. In these two articles, the adsorption and photocatalytic process were both fitted to pseudo-first order kinetics and the degradation efficiency was dominated by photocatalysis step. Additionally, photocatalysis of composite titania particles in aqueous solution is not only related to surface area, pore structure and adsorption amount, more importantly, but also decided by active components mass, crystallite size and phase composition.

3.5. Separation and Durability test

Last question that needs to be answered is the catalyst separation and durability. Thus, five consecutive cycles were performed with TD-1.5 as catalyst for RhB degradation. At the beginning, 0.05 g of TD-1.5 was dispersed in 100 ml of RhB solution with 10 mg/l. The suspension underwent five consecutive cycles under 250W UV-light irradiation, each testing for 1 h. After each cycle, we settled down the suspension for 0.5 h and found that the hybrid TiO_2/diatomite catalyst was precipitated much more quickly than P25 as shown in **Fig. 6a** because of the micron-sized diatomite support. And then the catalyst was separated by suction filtration, washed with ethanol and deionized water, dried in air at 105℃ for 4 h, and reused in the next cycle. The result of five consecutive cycles is shown in **Fig. 6b**, after five repeated experiments under same condition, the catalyst still maintained a relatively high activity. From the first run to the last, the degradation efficiency of RhB was only decreased from 99.6% to 74.7%. Such a decline in the ratio of RhB degradation could be ascribed to a gradual mass loss of catalyst for sampling, filtrating and washing.

Conclusions

In summary, disk-like TiO_2/diatomite hybrid photocatalysts were synthesized by a modified sol-gel method and following calcination route. This material was composed of natural porous mineral with good adsorption capacity and titanium dioxide with high photocatalytic activity. The effect of TBOT dosage on the photoactivity of the TiO_2/diatomite composite was studied. With the increasing TBOT dosage, the degradation efficiency of RhB first increased and then decreased. It demonstrates that the TBOT dosage is an important factor of this immobilized TiO_2 photocatalyst. The photocatalytic degradation of RhB over TiO_2/diatomite hybrid catalyst in aqueous suspension was found to follow pseudo-first order kinetics according to the Langmuir-Hinshelwood model. Furthermore, the diatomite

support not only impeded the TiO_2 particle agglomeration and phase transformation from anatase to rutile but also allowed this hybrid catalyst to be separated easily after treatment. The method proposed to prepare the immobilized TiO_2 photocatalyst can prevent the porous structure of diatomite from blocking by TiO_2 aggregations. This may provide a new route to prepare advanced immobilized photocatalytic materials using non-metal minerals as support.

Acknowledgements

This work was supported by National Technology R&D Program in the 12th five years plan of China (2011BAB03B07). The first author acknowledges China Scholarship Council (CSC) for financial support. The authors would also like to thank to Professor Ian R. Gentle from School of Chemistry and Molecular Biosciences, The University of Queensland for suggestion and assistance with this experiment.

Reference

[1] M.R. Hoffmann, S.T. Martin, W. Choi, D.W. Bahnemann, Environmental applications of semiconductor photocatalysis, Chem. Rev. 95 (1995) 69-96.

[2] A. Fujishima, T.N. Rao, D.A. Tryk, Titanium dioxide photocatalysis, J. Photochem. Photobiol., C 1 (2000) 1-21.

[3] X. Chen, Titanium dioxide nanomaterials: Synthesis, properties, modifications, and applications, Chem. Rev. 107 (2007) 2891-2959.

[4] J. Mo, Y. Zhang, Q. Xu, J.J. Lamson, R. Zhao, Photocatalytic purification of volatile organic compounds in indoor air: A literature review, Atmos. Environ. 43 (2009) 2229-2246.

[5] L. Andronic, D. Perniu, A. Duta, Synergistic effect between TiO_2 sol-gel and Degussa P25 in dye photodegradation, J. Sol-Gel Sci. Technol. 66 (2013) 472-480.

[6] X. Meng, Z. Qian, H. Wang, X. Gao, S. Zhang, M. Yang, Sol-gel immobilization of SiO_2/TiO_2 on hydrophobic clay and its removal of methyl orange from water, J. Sol-Gel Sci. Technol. 46 (2008) 195-200.

[7] L. Zou, Y. Luo, M. Hooper, E. Hu, Removal of VOCs by photocatalysis process using adsorption enhanced TiO_2-SiO_2 catalyst, Chem. Eng. Process. 45 (2006) 959-964.

[8] Y. Lu, D. Wang, C. Ma, H. Yang, The effect of activated carbon adsorption on the photocatalytic removal of formaldehyde, Build. Environ. 45 (2010) 615-621.

[9] V. Durgakumari, M. Subrahmanyam, K.V. Subba Rao, A. Ratnamala, M. Noorjahan, K. Tanaka, An easy and efficient use of TiO_2 supported HZSM-5 and TiO_2+HZSM-5 zeolite combinate in the photodegradation of aqueous phenol and p-chlorophenol, Appl. Catal., A 234 (2002) 155-165.

[10] D. Kibanova, J. Cervini-Silva, H. Destaillats, Efficiency of clay-TiO_2 nanocomposites on the photocatalytic elimination of a model hydrophobic air pollutant, Environ. Sci. Technol. 43 (2009) 1500-1506.

[11] D. Kibanova, M. Sleiman, J. Cervini-Silva, H. Destaillats, Adsorption and photocatalytic oxidation of formaldehyde on a clay-TiO_2 composite, J. Hazard. Mater. 211-212 (2012) 233-239.

[12] H. Destaillats, D. Kibanova, M. Trejo, H. Destaillats, J. Cervini-Silva, Synthesis of hectorite-TiO_2 and kaolinite-TiO_2 nanocomposites with photocatalytic activity for the degradation of model air pollutants, Appl. Clay Sci. 42 (2009)563-568.

[13] M. Rafatullah, O. Sulaiman, R. Hashim, A. Ahmad, Adsorption of methylene blue on low-cost adsorbents: A review, J. Hazard. Mater. 177 (2010) 70-80.

[14] X.-Y. Chuan, X.-Ch. Lu, X.-Chu Lu, Photodecomposition of methylene blue by TiO_2-mounted diatomite, J. Inorg. Mater. 23 (2008) 657-661.

[15] L. Cheng, Y. Kang, G. Li, Effect factors of benzene adsorption and degradation by nano-TiO_2 immobilized on diatomite, J. Nanomaterials 2012 (2012) 6-6.

[16] Z. Sun, C. Bai, S. Zheng, X. Yang, R.L. Frost, A comparative study of different porous amorphous silica minerals supported TiO_2 catalysts, Appl. Cataly. A 458 (2013) 103-110.

[17] X. He, A. Tang, H. Yang, J. Ouyang, Synthesis and catalytic activity of doped TiO_2-palygorskite composites, Appl. Clay Sci. 53 (2011) 80-84.

[18] C. Huo, H. Yang, Preparation and enhanced photocatalytic activity of Pd-CuO/palygorskite nanocomposites, Appl. Clay Sci. 74 (2013) 87-94.

[19] F. Akhtar, Y. Rehman, L. Bergström, A study of the sintering of diatomaceous earth to produce porous ceramic monoliths with bimodal porosity and high strength, Powder Technol. 201 (2010) 253-257.

[20] Z. Sun, X. Yang, G. Zhang, S. Zheng, R.L. Frost, A novel method for purification of low grade diatomite powders in centrifugal fields, International Journal of Mineral Processing, 125 (2013) 18-26.

[21] C.-T. Hsieh, W.-S. Fan, W.-Y. Chen, J.-Y. Lin, Adsorption and visible-light-derived photocatalytic kinetics of organic dye on Co-doped titania nanotubes prepared by hydrothermal synthesis, Sep. Purif. Technol. 67 (2009) 312-318.

[22] K. Lv, J. Yu, K. Deng, J. Sun, Y. Zhao, D. Du, M. Li, Synergistic effects of hollow structure and surface fluorination on the photocatalytic activity of titania, J. Hazard. Mater. 173 (2010) 539-543.

[23] J. Zhao, T. Wu, K. Wu, K. Oikawa, H. Hidaka, N. Serpone, Photoassisted degradation of dye pollutants. 3. Degradation of the cationic dye Rhodamine B in aqueous anionic surfactant/TiO_2 dispersions under visible light irradiation: Evidence for the need of substrate adsorption on TiO_2 particles, Environ. Sci. Technol. 32 (1998) 2394-2400.

[24] Q. Wang, C. Chen, D. Zhao, W. Ma, J. Zhao, Change of adsorption modes of dyes on fluorinated TiO_2 and its effect on photocatalytic degradation of dyes under visible irradiation, Langmuir, 24 (2008) 7338-7345.

[25] Y. Jia, W. Han, G. Xiong, W. Yang, Layer-by-layer assembly of TiO_2 colloids onto diatomite to build hierarchical porous materials, J. Colloid Interface Sci. 323 (2008) 326-331.

[26] C.G. Silva, J.L. Faria, Effect of key operational parameters on the photocatalytic oxidation of phenol by nanocrystalline sol-gel TiO_2 under UV irradiation, J. Mol. Catal. A: Chem. 305 (2009) 147-154.

[27] Z. Sun, S. Zheng, G.A. Ayoko, R.L. Frost, Y. Xi, Degradation of simazine from aqueous solutions by diatomite-supported nanosized zero-valent iron composite materials, J. Hazard. Mater. 263, Part 2 (2013) 768-777.

[28] H. Khan, D. Berk, Sol-gel synthesized vanadium doped TiO_2 photocatalyst: physicochemical properties and visible light photocatalytic studies, J. Sol-Gel Sci. Technol. 68 (2013) 180-192.

[29] K. Farhadian Azizi, M.M. Bagheri-Mohagheghi, Transition from anatase to rutile phase in titanium dioxide (TiO_2) nanoparticles synthesized by complexing sol-gel process: effect of kind of complexing agent and calcinating temperature, J. Sol-Gel. Sci. Technol. 65 (2013) 329-335.

[30] A. Molea, V. Popescu, N.A. Rowson, A.M. Dinescu, Influence of pH on the formulation of TiO_2 nano-crystalline powders with high photocatalytic activity, Powder Technol. 253 (2014) 22-28.

[31] K.-J. Hsien, W.-T. Tsai, T.-Y. Su, Preparation of diatomite-TiO_2 composite for photodegradation of bisphenol-A in water, J. Sol-Gel Sci. Technol. 51 (2009) 63-69.

[32] K.-J. Hwang, J.-W. Lee, W.-G. Shim, H.D. Jang, S.-I. Lee, S.-J. Yoo, Adsorption and photocatalysis of nanocrystalline TiO_2 particles prepared by sol-gel method for methylene blue degradation, Adv. Powder Technol. 23 (2012) 414-418.
[33] I. Konstantyinou, T. Albanis, TiO2-assisted photocatalytic degradation of azo dyes in aqueous solution: kinetic and mechanistic investigations, A review, Appl. Catal. B 49 (2004) 1-14.
[34] H. Liu, Z. Lian, X. Ye, W. Shangguan, Kinetic analysis of photocatalytic oxidation of gas-phase formaldehyde over titanium dioxide, Chemosphere 60 (2005) 630-635.
[35] W.C. Hao, S.K. Zheng, C. Wang, T.M. Wang, Comparison of the photocatalytic activity of TiO_2 powder with different particle size, J. Mater. Sci. Lett. 21 (2002) 1627-1629.
[36] C.-H. Liang, F.-B. Li, C.-S. Liu, J.-L. Lü, X.-G. Wang, The enhancement of adsorption and photocatalytic activity of rare earth ions doped TiO_2 for the degradation of Orange I, Dyes Pigment. 76 (2008) 477-484.

Figure captions:

Fig.1 Flow chart of the synthesis of TiO_2/diatomite hybrid catalysts by sol-gel method

Fig.2 SEM micrographs of (a) raw diatomite, (b) purified diatomite (DE), (c-f) TD-X samples with X=0.5, 1.5, 2.0 and 3.0. ***Inset*** illustrates the EDX results of surface-distribution scanning (blue points represent element Ti)

Fig. 3 (a) Nitrogen adsorption/desorption isotherms and **(b)** corresponding BJH pore size distribution curve of DE and hybrid TiO_2/diatomite containing different TBOT dosage

Fig.4 XRD patterns of DE, pure TiO_2 without support and hybrid TiO_2/diatomite containing different TBOT dosage calcined at 750 ℃

Fig.5 (a) The decrease in the concentration of RhB by the hybrid TiO_2/diatomite catalysts and Degussa P25 under UV-light irradiation. **(b-c)** The dependence of photodegradation efficiency on irradiation time and pseudo-first order plots for the catalysts. **(d)** The variation tendency of rate constant and equilibrium adsorption amount versus TBOT dosage for different TiO_2/diatomite samples

Fig.6 (a) Digital photograph of settling rate compared between as-prepared TD-1.5 particles and Degussa P25. **(b)** Stability of as-prepared TD-1.5 catalyst for the photodegradation of RhB aqueous solution under UV-light (λ **>** 365 nm) irradiation

Fig.1

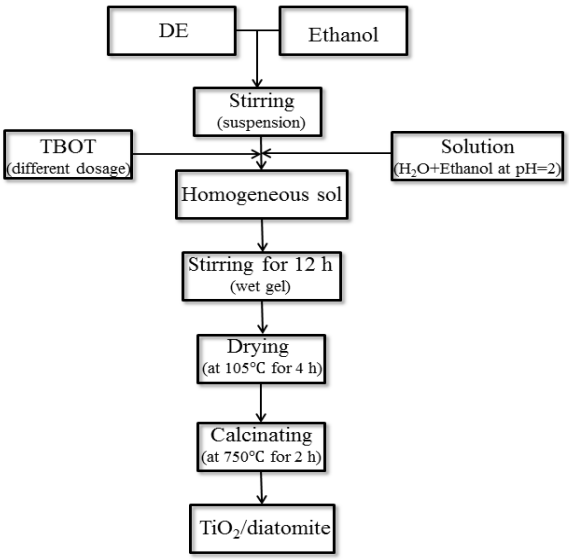

Fig.2

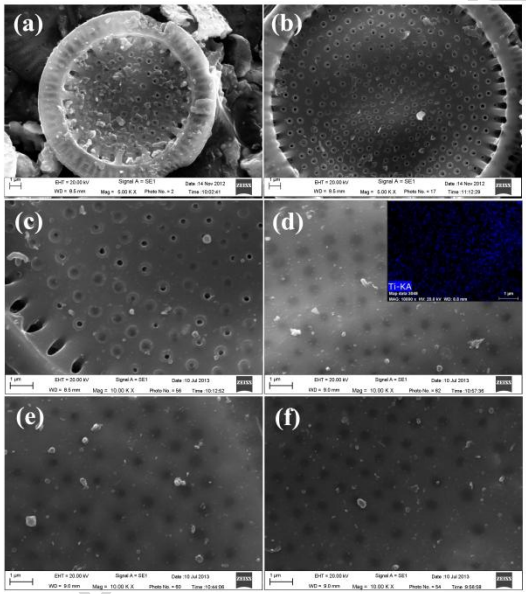

Fig.3(a)

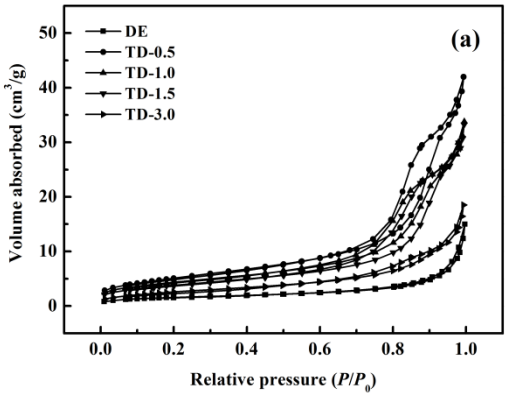

Fig.3(b)

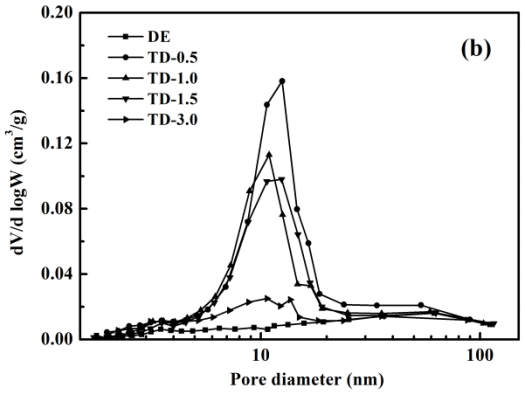

Fig.4

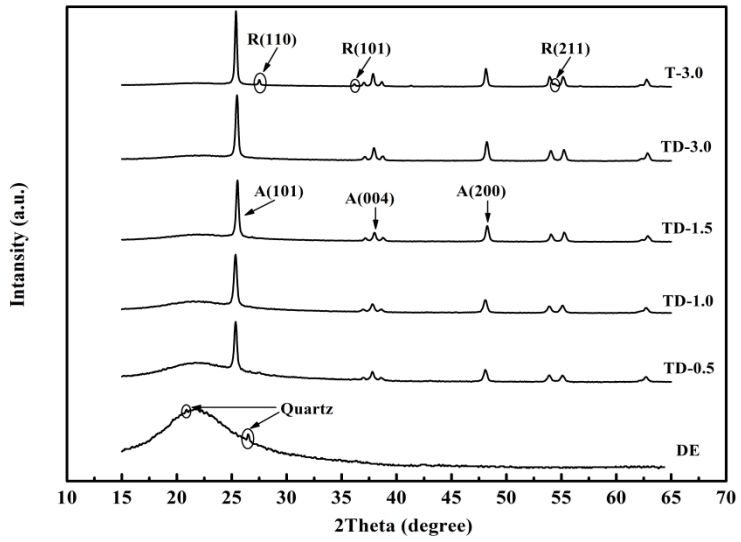

Fig.5(a)

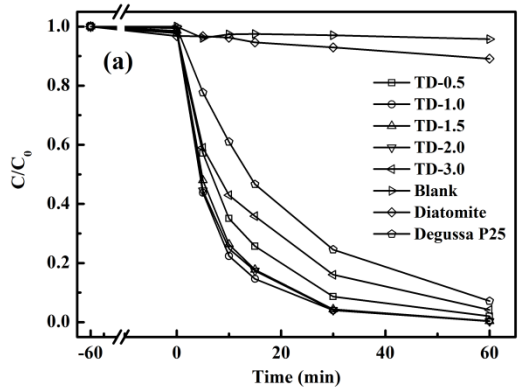

Fig.5(b)

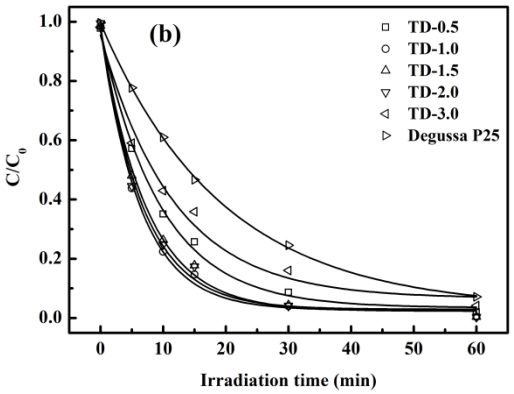

Fig.5(c)

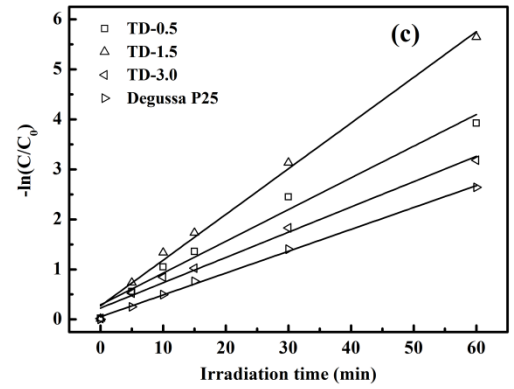

Fig.5(d)

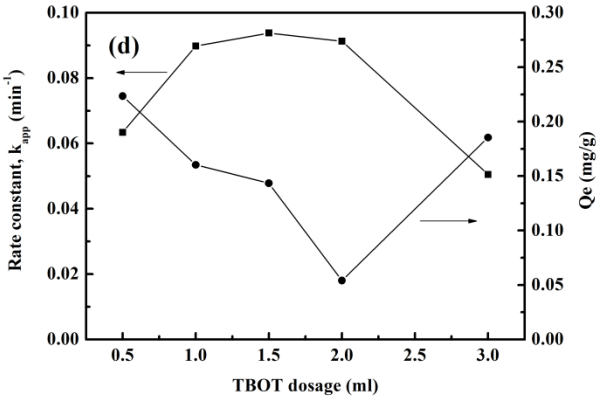

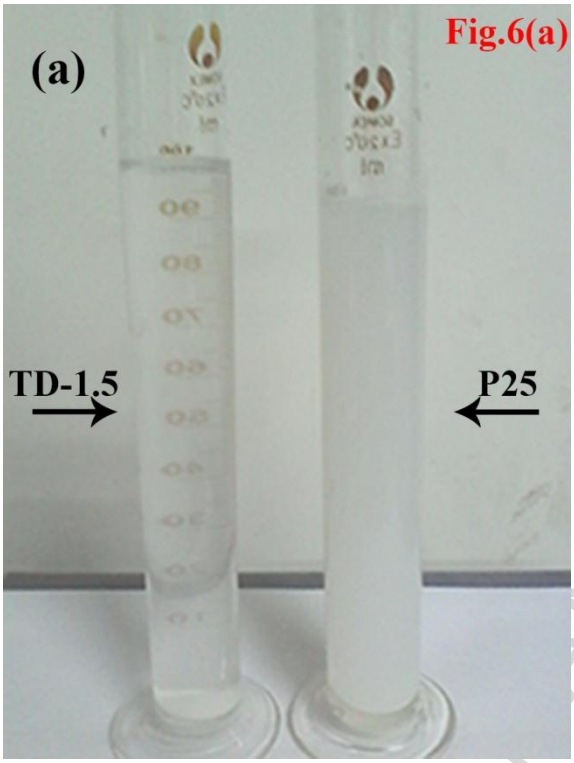

Fig.6(b)

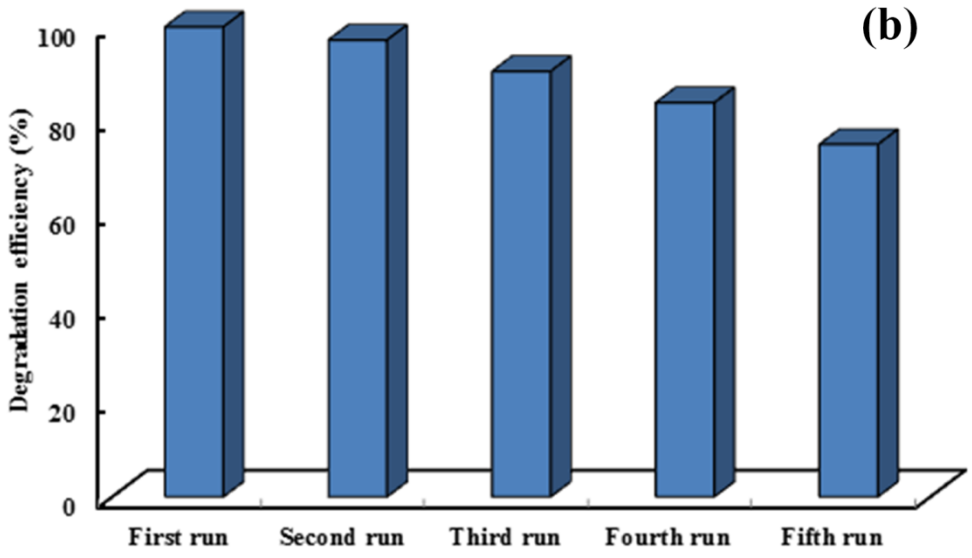

Graphical Abstract

TiO_2 nanoparticles were immobilized onto purified diatomite using a modified sol-gel method. The morphology of the as-prepared TiO_2/diatomite hybrid catalyst is shown in the illustration. The effect of titanium (IV) butoxide dosage on degradation efficiency for dye Rhodamine B under UV-light irradiation was investigated, as well as durability.

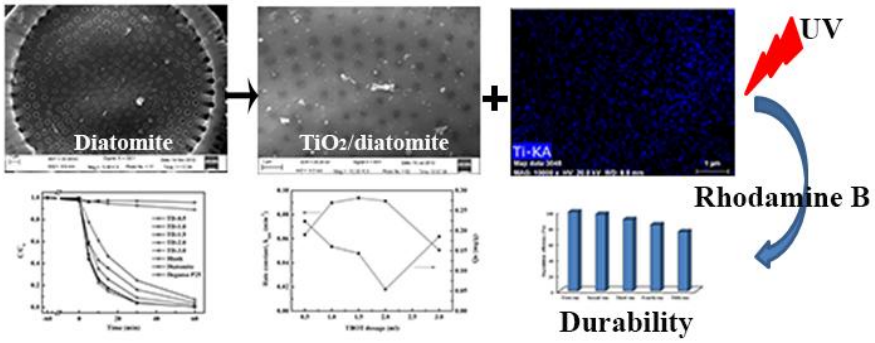

Dear Editor,

The research highlights of this manuscript are as follows:

- The optimum loading dosage of TiO_2 on nano-TiO_2/diatomite hybrid catalyst was investigated.
- The as-prepared composites were characterized by SEM/EDX, XRD and N_2-adsorption instrument.
- The effect of titanium butoxide dosage and diatomite support on degradation was investigated.
- The adsorption and photocatalysis for Rhodamine B in water were studied.
- Nano-TiO_2/diatomite hybrid catalyst shown potential prospects in environmental remediation.

Table 1

Chemical constituent of the purified diatomite (DE)

Constituent	SiO_2	Al_2O_3	Fe_2O_3	CaO	MgO	Na_2O	L.O.I.[a]
(%)	91.74	2.76	1.14	0.34	0.21	0.12	3.52

[a] Loss on ignition

Table 2

EDX results of percentile composition both in weight and atomic of oxygen, silicon and titanium in TD-X

Samples / Elements	TD-0.5		TD-1.5		TD-2.0		TD-3.0	
	Weight%	Atomic%	Weight%	Atomic%	Weight%	Atomic%	Weight%	Atomic%
O K	45.81	60.13	54.64	68.57	48.24	63.19	43.13	58.48
Si K	52.12	38.97	41.97	30.01	45.92	34.26	49.33	38.10
Ti K	2.07	0.91	3.39	1.42	5.83	2.55	7.54	3.41
Total	100	100	100	100	100	100	100	100

Table 3

Summary of crystalline size of $A_{(101)}$ calculated from XRD plots and surface characteristics of DE and TD-X samples determined from N_2 sorption at -196 ℃

Sample	Crystalline size of $A_{(101)}$ (nm)	BET Surface area $(m^2/g)^a$	Pore volume $(cm^3/g)^b$	Average pore diameter $(nm)^c$
DE		5.57	0.023	17.77
TD-0.5	14.65	18.84	0.065	11.59
TD-1.0	16.17	15.65	0.052	11.32
TD-1.5	18.29	13.84	0.052	11.83
TD-3.0	23.73	9.62	0.028	11.23

[a] specific surface area data calculated from the multi-point BET method;

[b] pore volume obtained from the BJH desorption cumulative volume of pores between 17.000 and 3000.000 width;

c average pore diameter estimated from the desorption isotherm by the BJH model;

Table 4

Summary of the pseudo-first order kinetics and degradation efficiency of hybrid TiO_2/diatomite catalysts under UV-light (λ **>** 365 nm) irradiation for 1 h

Samples	Apparent rate constant (min^{-1})	R^2	Degradation efficiency (%)
TD-0.5	0.0634	0.97538	98.0
TD-1.0	0.0898	0.98395	99.6
TD-1.5	0.0938	0.99253	99.7
TD-2.0	0.0913	0.99254	99.7
TD-3.0	0.0505	0.98555	95.9
Degussa P25	0.0437	0.99771	98.2